Glycobiology Advance Access published July 3, 2012



# *Burkholderia cenocepacia* lectin A binding to heptoses from the bacterial lipopolysaccharide.

**Roberta Marchetti[2,*], Lenka Malinovska[3,*], Emilie Lameignère[4], Lenka Adamova[3], Cristina de Castro[2], Gianluca Cioci[5], Christian Stanetty[6], Paul Kosma[6], Antonio Molinaro[2], Michaela Wimmerova[3], Anne Imberty[1,4] and Alba Silipo[1,2]**

[2]Dipartimento di Scienze Chimiche, Università di Napoli "Federico II", Napoli, Italy. [3]National Centre for Biomolecular Research and Department of Biochemistry, Faculty of Science, Masaryk University, Brno, Czech Republic. [4]CERMAV-CNRS- UPR5301 affiliated to Université de Grenoble, France. [5]ESRF, Grenoble, France. [6]Department of Chemistry, University of Natural Resources and Applied Life Sciences, Vienna, Austria.

[1]To whom correspondence should be addressed: Tel: +39 081 674 146, Fax: +39 081 674 393; e-mail: silipo@unina.it (A.S.); Tel: +33-476-037-636, Fax: +33-476-547-203; : e-mail: anne.imberty@cermav.cnrs.fr (A.I.)

* These two authors contributed equally to the publication.

**Abstract**

Bacteria from the *Burkholderia cepacia* complex (Bcc) cause highly contagious pneumonia among cystic fibrosis (CF) patients. Among them, *Burkholderia cenocepacia* is one of the most dangerous in the Bcc and is the most frequent cause of morbidity and mortality in CF patients. Indeed, it is responsible of "cepacia syndrome", a deadly exacerbation of infection, that is the main cause of poor outcomes in lung transplantation. *B. cenocepacia* produces several soluble lectins with specificity for fucosylated and mannosylated glycoconjugates. These lectins are present on the bacterial cell surface and it has been proposed that they bind to lipopolysaccharide epitopes. In this work, we report on the interaction of one *B. cenocepacia* lectin, BC2L-A, with heptose and other *manno* configured sugar residues. Saturation Transfer Difference (STD) NMR spectroscopy studies of BC2L-A with different mono- and disaccharides demonstrated the requirement of *manno* configuration with hydroxyl or glycol group at C6 for the binding process. The crystal structure of BC2L-A complexed with the methyl-heptoside confirmed the location of the carbohydrate ring in the binding site and elucidated the orientation of the glycol tail, in agreement with NMR data. Titration calorimetry performed on monosaccharides, heptose disaccharides and bacterial heptose-containing oligosaccharides and polysaccharides confirmed that bacterial cell wall contains carbohydrate epitopes that can bind to BC2L-A. Additionally, the specific binding of fluorescent BC2L-A lectin on *B. cenocepacia* bacterial surface was demonstrated by electron microscopy.

*Keywords*: bacterial lectin, NMR, heptose, lipopolysaccharide, titration microcalorimetry

## Introduction

*Burkholderia cenocepacia* and *Pseudomonas aeruginosa* are both pathogenic bacteria involved in chronic lung infections, especially in cystic fibrosis patients (Govan and Deretic, 1996). In order to adhere to host tissues, as a part of their invasion strategy, these pathogens use oligosaccharide-mediated recognition processes. These two bacteria species present carbohydrate binding proteins on the flagellum and fimbriae as well as soluble lectins conjugated to the bacterial cell surface or located in the extracellular matrix (Imberty and Varrot, 2008, Imberty *et al.*, 2004, Imberty *et al.*, 2006). *P. aeruginosa* contains two soluble lectins, PA-IL and PA-IIL, with specificities for galactosides and fucosides respectively (Gilboa-Garber, 1982). These lectins are virulence factors as established in a murine model of lung infection (Chemani *et al.*, 2009). In *B. cenocepacia,* three soluble lectins have been identified, BC2L-A, BC2L-B and BC2L-C, all containing a PA-IIL like domain, while in two of them there is an additional N-terminal domain without any similarities with known proteins (Lameignere *et al.*, 2008, Šulák *et al.*, 2010, Šulák *et al.*, 2011). The smallest *B. cenocepacia* lectin is BC2L-A that displays mannose specificity (Lameignere *et al.*, 2008). Each monomer of 13.8 kDa contains one carbohydrate recognition domain which includes two $Ca^{2+}$ ions directly involved in ligand binding. Crystal structures obtained in presence of α-methyl-mannoside (αMeMan) (Lameignere *et al.*, 2008) and branched trimannoside (Lameignere *et al.*, 2010) demonstrated that the strong affinity ($K_d$ = 2.7 μM for αMeMan) is related to the coordination of three mannose hydroxyl groups, namely O-2, O-3 and O-4 by the two calcium ions in the binding site. Such involvement of a pair of calcium ions in carbohydrate binding has only been observed for the related lectin PA-IIL from *P. aeruginosa* (Mitchell *et al.*, 2002), CV-IIL from *Chromobacterium violaceum* (Pokorná *et al.*, 2006) and RS-IIL from *Ralstonia solanacearum* (Sudakevitz *et al.*, 2004). These three lectins assembled as tetramers while the *Burkholdera* lectins BC2L-A and the lectin C-terminal domain of BC2L-C are dimeric (Lameignere *et al.*, 2008, Šulák *et al.*, 2011).

Attempts to determine the localization of *Burkholderia* lectins concluded that the three lectins are secreted or released into the extracellular medium (Šulák *et al.*, 2011). BC2L-B and -C lectins are specifically released from the intact cells upon mannose treatment suggesting that an important portion is attached to the external envelope of bacteria. BC2L-A was not detected on the surface, but this may be due to its much lower expression level in *B. cenocepacia* (Lameignere *et al.*, 2008). It was further demonstrated that BC2L-C binds efficiently to L-*glycero*-D-*manno*-heptose (L,D-Hep) (Šulák *et al.*, 2011) an abundant

component of the *B. cenocepacia* lipopolysaccharide (LPS) (De Soyza *et al.*, 2008). Heptoses are very important residues basically present as components of the core region of LPS from Gram-negative bacteria, covalently linked to the Kdo-lipid A portion (Silipo and Molinaro, 2010). In the case of enterobacterial LPS, a heptose trisaccharide fragment: α-L,D-Hep*p*$^{III}$-(1-7)-α-L,D-Hep*p*$^{II}$-(1-3)-α-L,D-Hep*p*$^{I}$) is always present in the inner core region of LPS (Holst, 2007). In *Burkholderia*, heptose is ubiquitous and found in different glycosidic linkages and in higher amount than in *Enterobacteriaceae* (De Soyza *et al.*, 2008). In addition to or instead of L,D-Hep, some LPS may contain D-*glycero*-D-*manno*-heptose (D,D-Hep) which is the biosynthetic precursor of L,D-Hep. In a limited number of cases, heptoses have also been detected as components of repeating units of O-antigens, such as in *Yokenella regensburgei* (Kosma, 2008), whereas in a strain of *Agrobacterium tumefaciens* L,D-Hep is the only LPS O-antigen carbohydrate component (De Castro *et al.*, 2004).

Interaction between plant lectins and LPS has been proposed to play a role in the establishment of symbiosis between legume plants and nitrogen-fixing bacteria (Agrawal *et al.*, , Jayaraman and Das, 1998). The interaction between human lectins of the innate immune system, such as surfactant protein D (SP-D) and mannan-binding protein (MBP), and pathogenic bacteria is mediated by heptose (Kawasaki *et al.*, 1989, Wang *et al.*, 2008). In *P. aeruginosa* and *B. cenocepacia*, bacterial lectins interact with LPS heptose on the cell surface and participate in host tissue binding and/or colony aggregation (Šulák *et al.*, 2011). Despite of these important roles, the number of investigations on lectin-heptose interaction is very small. Heptose has been demonstrated to bind efficiently to Concanavalin A, a classical mannose specific lectin (Jaipuri *et al.*, 2008) and the crystal structure of surfactant protein D has been solved in complex with heptoses of both L-*glycero*- and D-*glycero*-D-*manno*-configuration via the side chain or ring hydroxyl groups, respectively (Wang *et al.*, 2008).

In this work we report the interaction of BC2L-A with heptose and other *manno* configured sugar residues by a combination of structural and thermodynamic approaches. Saturation Transfer Difference (STD) NMR spectroscopy studies of BC2L-A with different mono- and disaccharides containing residues with *manno* configuration were performed in order to shed light on its recognition properties. A crystal structure of BC2L-A complexed with the methyl-heptoside confirms the orientation of the *manno* configured ring in the binding site and the coordination to calcium ions. Titration calorimetry indicates that the the α-L,D-Hep-(1-7)-α-L,D-Hep disaccharide and a [α-L,D-Hep-(1-7)]$_n$ polysaccharide are high affinity ligands, and that BC2L-A binds to LPS derived from different *Burkholderia*. Microscopy study confirmed the binding of fluorescent lectin on bacterial surface and in biofilms. We demonstrate here for the first time that a soluble lectin from *Burkholderia cenocepacia* displays affinity for heptose and heptose-containing oligo and polysaccharides and can therefore attach to the outer membrane of Burkholderia cells.

## Results and Discussion

### Epitope mapping of monosaccharides bound to BC2L-A

The analysis of the binding of carbohydrate ligands to BC2L-A was performed by one-dimensional STD-NMR experiments (Mayer and Meyer, 2001), in which the receptor protein is selectively saturated. At long irradiation times, the saturation is transferred to the bound ligand, first to the protons belonging to the ligand epitope, giving rise to signal enhancements stronger for the protons in closest proximity with the protein (Meyer and Peters, 2003). STD NMR data obtained from D-mannose (Figure 1, see also table S1 in supplemental material) and the corresponding α-methyl glycoside (data not shown) show that all protons of the monosaccharide exhibit some degree of enhancement, demonstrating binding of the mannose to the protein. Indeed, the monosaccharide occupy all the binding pocket of the protein and therefore all carbohydrate ring hydrogens are close to receptor atoms and give rise to STD signals. The most prominent STD signals were observed for H-2, H-3 and H-4 protons, all strongly involved in the binding, while the anomeric protons were slightly visible. These data are in agreement with the crystal structures of BC2L-A complexed with αMeMan (Lameignere *et al.*, 2008). The mannose binding pocket is rather deep, and all ring hydrogens are close to protein atoms. Hydrogens at C-5 and C-6 are close to His112 but this residue

displays conformational flexibility, which may explain why the saturation transferred to this proton is not as efficient as for the other ones.

In order to investigate the effect of different groups at C-5, STD-NMR experiments were conducted on methyl glycoside of α-L,D-Hep (αMeHep) **2** that presents a glycol group at C-5 (Scheme 1) and *O*-methyl rhamnosides with a methyl group at C-5. Figure 2 shows $^{1}$H and 1D STD NMR spectra obtained with αMeHep **2** (see also Table S2 in supplemental material). By comparing the STD spectrum with its corresponding reference experiment, it could be clearly inferred that the monosaccharide was able to bind to BC2L-A, as shown by the enhancement of several signals. In fact, the epitope mapping revealed that, beside the expected interacting H-2, H-3 and H-4 proton signals, the region comprising H-5/ H-7 was close to the receptor and contributed to the overall binding. Further STD NMR experiments were carried out to investigate the direct binding of 6-deoxy-sugars to BC2L-A, confirming that the terminal ring protons represented a structural requirement for binding to the lectin. In fact, the STD spectrum obtained with methyl-α-D-rhamnoside did not display signals (Figure S1 and table S3 in supplemental material) indicating that the interaction is much weaker when no hydroxyl groups are present on position 6. No STD signals were observed for the interaction of BC2L-A with L-rhamnose (Figure S2 and Table S3 in supplemental material), that exists in the $^{1}C_{4}$ chair in solution.

**Epitope mapping of disaccharides bound to BC2L-A**

We have also analyzed the interaction between the protein and disaccharides containing L-*glycero*-D-*manno* heptoses. In Figures 3 and S3 (suppl. material), STD NMR spectra performed using α-L,D-Hep-(1-7)-α-L,D-Hep (**5**) and α-L,D-Hep-(1-3)-α-L,D-Hep (**4**) disaccharides have been reported. In both cases, the observed line broadening was attributable to an increased relaxation rate of the protein-ligand complex, as an indication that the disaccharides were in contact with the receptor. For α-L,D-Hep-(1-3)-α-L,D-Hep **4** (Figure 3), due to a significant spectral overlap, a quantitative analysis of the STD signal intensities was difficult whereas 2D STD NMR experiments were impaired by physical characteristic of protein, such as its low molecular weight.

Nevertheless, from a qualitative analysis of the spectrum, performed comparing the STD NMR spectrum with its corresponding reference, it was evident that H-5, H-4 and H-3 protons, belonging to ring **A** and almost overlapping, were those receiving highest transfer of magnetization and are thus strongly involved in the interaction. Results obtained from a

quantitative analysis performed on the α-L,D-Hep-(1-7)-α-L,D-Hep **5** indicated that the largest fraction of saturation in the disaccharide moiety was received by protons H-6 and H-7 (Figure S3 in supplemental material). In both disaccharides, it can be therefore concluded that the non reducing unit is the one that plays the stronger role in the binding event.

**Crystal structure of BC2L-A complexed with αMeHep 2**

Crystals of BC2L-A complexed with αMeHep have been obtained by co-crystallization with space group $C222_1$. The structure solved at 2.7 Å resolution demonstrates the presence of two and a half dimers per asymmetric unit. The overall crystal structure and the dimer arrangements (Figure 4a) are very similar to the previously described complex between BC2L-A and αMeMan (Lameignere *et al.*, 2008) and will not be described further.

The N-term region is poorly resolved into the electron density and has been omitted from the final model. Clear electron density for one molecule of αMeHep and two calcium ions is observed in each binding site (Figure 4b). As observed in other crystal structures of PAIIL-related lectins, three hydroxyl groups of the sugar ring are engaged in coordination contact with the two calcium ions with O...Ca distances varying from 2.35 to 2.65 Å. A dense network of hydrogen bonds involves the O2, O3, O4 and O6 hydroxyl groups of heptose and amino acids Asn28, Glu31, Asp110, Asp113, Asp115, Asp118 as well as terminal carboxylate of Gly128 of neighboring monomer. The ring heptose oxygen O5 receives one hydrogen bond from Ala30 main chain nitrogen.

The glycol side chain of heptose establishes two hydrogen bonds involving hydroxyl group O6 with side chain of Asp110 and main chain nitrogen of Glu31. This hydrogen bond network is similar to what has been observed in BC2L-A/αMeMan complexes and corresponds to a conformation of the ω1 torsion angles (O5-C5-C6-O6) close to -40°, corresponding to energetically favored *gauche-gauche* conformation (gg) according to Marchessault and Pérez (Marchessault and Pérez, 1979). The hydroxyl group O7 of the glycol chain does not establish hydrogen bonds and can adopt a variety of conformations for ω2 (O6-C6-C7-O7) ranging to -78° to 102° (Table S6). However, in most monomers, the C7 carbon is close to His112 and this part of the glycol can participate in stabilization. This His112 is observed in two conformations in monomers A, C and D that could be described as “closed” with His ring close to both C6 and O1 heptose atoms, and “open” with His ring close only to the glycol group (Figure 4b and 4c). In monomers B and E, the “close” conformation is the only one observed.

**Affinity measurements and thermodynamics by titration microcalorimetry.**

L,D-Heptose and derivatives were tested by titration microcalorimetry in order to determine the affinity for BC2L-A (Table 2). In all cases, the interaction results in exothermic peaks as displayed on the examples in Figure 5. All curves could be fitted with a one-site model, although the binding of the reducing monosaccharide L,D-heptose shows some cooperativity between the two monomers, as previously described for mannose binding (Lameignere *et al.*, 2008). The reducing monosaccharide displays medium range affinity ($K_d$ = 137 μM), while the introduction of a methyl group in α-configuration enhances the affinity ($K_d$ = 53.8 μM). The configuration of the glycol tail is crucial, since the D,D-heptose monosaccharide is not recognized by BC2L-A

The α1-3 and α1-7 linked disaccharides behave approximately as the αMeHep **2** monosaccharides, with a slightly higher affinity of BC2L-A for the Hep α1-7 Hep disaccharide. The α-methyl derivative of this disaccharide (**6**) is the best ligand of this series with a $K_d$ of 18 μM. The observed affinity for heptose residues is one order of magnitude weaker to what was observed for the binding of BC2L-A to αMeMan (Lameignere *et al.*, 2008).

Analysis of the thermodynamic contribution to the free energy of binding demonstrates a favourable role of the entropy term, with negative values of -TΔS. The binding is equally driven by enthalpy and entropy term for the heptose monosaccharides and derivatives and is clearly entropy driven for the disaccharides. Such favorable entropy of binding is unusual for protein-carbohydrate interactions where a strong entropy barrier is generally observed (Dam and Brewer, 2002). This appears to be a signature of this two-calcium family of lectins since favorable entropy of binding has been observed for all of the members, with a particularly strong contribution for CV-IIL (Pokorná *et al.*, 2006).

BC2L-A was also tested for its ability to bind to major oligosaccharide fragments from *Burkholderia* LPS. Direct binding to whole LPS could not be observed by microcalorimetry, presumably because of solubility issue and/or accessibility of the heptose residues. When working with delipidated LPS, such as core oligosaccharides from *B. multivorans* and *B. cenocepacia*, a good affinity is observed with heptose-carrying oligosaccharides with $K_d$ in the range of 300 μM. Interestingly, BC2L-A can also interact with polysaccharides from other bacterial species. The linear polysaccharide from *Agrobacterium radiobacter* is a

homopolymer of α1-3 linked L,D-heptose residues. The stoichiometry of binding indicates that BC2L-A binds to only one residue in the whole polysaccharide, presumably the one at the non-reducing end since free O-3 is required for coordination of calcium ions in the lectin binding site. A strong affinity is observed ($K_d$ = 3 μM) with an enthalpy of binding significantly higher than for the mono or disaccharides, suggesting a structured conformation of the polysaccharides creating additional contacts with the protein.

**Binding of BC2L-A to surfaces of *Burkholderia cenocepacia***

BC2L-A labeled with FITC was used in order to determine its ability to bind to surfaces of *B. cenocepacia* LMG 16656 (J2315). Cells and biofilms were incubated with BC2L-A-FITC and examined using fluorescence microscope. A visible fluorescence at the cell surfaces was observed (Figure 6a). *Escherichia coli* strain BL21(DE3) was used as negative control and BC2L-A-FITC was not able to bind to and stain these cells. Observed fluorescence was minimal (Figure S4b in supplemental material). When mixed together, *B. cenocepacia* cells were clearly distinguished from *E. coli* by BC2L-A-FITC staining (Figure S4c in supplemental material). Experiments were performed also with *B. cenocepacia* biofilm scraped from cultivation flasks (Figure 6b) and with undisturbed biofilm growing directly on a microscope slide. Both *B. cenocepacia* biofilms also provided clear fluorescent signal and distribution of fluorescence within biofilms was uniform.

**Conclusion**

In this study, a sequence of advanced techniques such as NMR spectroscopy, X-ray crystallography and titration microcalorimetry has disclosed the binding and epitope patterns of LPS heptose and other *manno* configured sugar residues to the lectin BC2L-A, produced by the opportunistic pathogen *B. cenocepacia.* Both X-ray crystallography and titration calorimetry showed a good affinity of heptose(s) residues for the lectin, in particular of the non reducing end residue, which arranges the angles (O5-C5-C6-O6) to the energetically favored *gg* conformation. By titration microcalorimetry it was also possible to observe binding of the lectin to major oligosaccharides such as those deriving from R-LPS from two *Burkholderia* strains, and to an another bacterial polysaccharide fully composed of heptose residues. In accordance, STD NMR spectroscopy studies of BC2L-A with different mono- and disaccharides indicated that L-*glycero*-α-D-*manno*-heptosides and D-mannose were both in contact with the protein binding pocket. No STD signals were observed for the 6-deoxy-sugars L- and D-rhamnose, highlighting the inability of the protein to recognize and bind

substrates lacking hydroxyl groups on position 6, independently on the chair conformation ($^1C_4$ or $^4C_1$). These data were confirmed by STD NMR experiments on α-(1-3) and α-(1-7) heptose disaccharides, both present in the LPS of *Burkholderia*, in which the binding of the terminal heptose was more effective, testifying a major role in the interaction with the protein.

LPS are the major components of the outer membrane of Gram-negative bacteria and exert a variety of biological activities in animals and plants. Their biosynthesis is indispensable for growth and survival of Gram-negative bacteria and they comprise about 10-15% of the total molecules in bacterial outer membranes covering about 75% of bacterial surface area, thus they are exposed to the external environment. They represent a defensive barrier which helps bacteria to resist to antimicrobial compounds and environmental stresses and are involved in many aspects of host–bacterium interactions such as recognition, adhesion and colonization. Together with other indispensable microbial products they are taken by the host organism as hallmark of microbial presence, and are hence referred to as Microbe Associated Molecular Patterns. In this work we have demonstrated that a lectin secreted by *B. cenocepacia* is able to bind particular and peculiar saccharide residues present in the majority of LPS core oligosaccharides. This recognition can be pivotal in bacterial social life such as quorum sensing, exit from dormancy, formation of microcolony and/or any other processes in which the detection of specific bacterial strain is necessary.

## Material and Methods

### Materials

The recombinant protein BC2L-A was cloned and expressed using the procedure previously described (Lameignere *et al.*, 2008) using genomic DNA from *B. cenocepacia* strain J2315 obtained from the Czech Collection of Microorganisms at Brno, as a template. Production in *Escherichia coli* BL21(DE3) and purification on D-mannose-agarose column (Sigma-Aldrich, Saint Louis) were reported previously (Lameignere *et al.*, 2010). The protein was eluted by 10mM EDTA and dialyzed first against buffer with calcium and then against distilled water in order to remove residual sugars from the binding site.

Monosaccharides **1-3** and disaccharides **4-6** were prepared according to literature (Artner *et al.*, 2011, Brimacombe and Kabir, 1986, Paulsen *et al.*, 1991, Reiter *et al.*, 1999).

LPS core oligosaccharide fragments from *B. multivorans* and *B. cenocepacia,* and LPS heptose O-antigen were prepared by hydrolysis of LPS with 1% AcOH, 3h, 100°C and

purified as described previously (De Castro *et al.*, 2004, Ierano *et al.*, 2008, Ortega *et al.*, 2009).

**NMR spectroscopic analysis**

Experiments on the free ligands were recorded on a Bruker 600-MHz DRX equipped with a cryo probe at 283 K. Spectra were calibrated with internal [D4](trimethylsilyl)propionic acid sodium salt (TSP, 10 μM). All the samples were dissolved in deuterated 0.1M Tris/HCl buffer with 2 mM $CaCl_2$ (pH 7.5).

All ligand proton resonances were assigned by using COSY, TOCSY, NOESY, ROESY and HSQC experiments. $^1$H-NMR spectra were recorded with 32 K and 64 K data points. Double quantum-filtered phase-sensitive COSY spectra were performed by using data sets of 4096 x 512 (t1 x t2) points. Total Correlation Spectroscopy (TOCSY) spectra were performed with a spin lock time of 100 ms, by using data sets of 4096 x 256 points. Nuclear Overhauser enhancement spectroscopy (NOESY) and ROESY spectra were measured by using data sets of 4096 x 256 points; mixing times between 100 and 400 ms were used. In all homonuclear spectra the data matrix was zero-filled in the F1 dimension to give a matrix of 4096 x 2048 points and resolution was enhanced in both dimensions by a cosine-bell function before Fourier transformation. Heteronuclear single quantum coherence (HSQC) experiments were measured in the $^1$H-detected mode via single quantum coherence with proton decoupling in the $^{13}$C domain, by using data sets of 2048 x 256 points. Experiments were carried out in the phase-sensitive mode according to the method of States at al (States *et al.*, 1982).

For the bound ligands, STD NMR experiments were performed using protein-ligand molar ratio varied from 1:50 to 1:100 and saturation times between 0.5 s to 2.5 s were used; a T1ρ filter (50 ms spin-lock pulse) to eliminate the unwanted broad resonance signals of the protein was used. The off-resonance frequency was maintained at 40 ppm and the on resonance frequency (-0.7, 0.5, 6.8 ppm) falls in a region in which ligand signals are completely absent, that is necessary to avoid positive falses in the STD spectrum. A train of 40 Gaussian-shaped pulses of 50 ms each (1 ms delay between pulses, field strength of 60-65 db) was employed, with a total saturation time of the protein envelope of 2 s. Saturated and reference spectra were acquired simultaneously by creating a pseudo-2D experiment. Reference experiments were carried out to assure the absence of direct irradiation of the ligand. STD spectra were performed with 16 K and 32 K data points. The original FID was zero-filled to 64 k and Fourier transformation with use of an exponential window function was applied. In all cases, the STD effect was calculated by $(I_0 - I_{sat})/I_0$, where $(I_0 - I_{sat})$ is the intensity of the signal in

the STD NMR spectrum and $I_0$ is the peak intensity of an unsaturated reference spectrum (off-resonance). The STD signal with the highest intensity was set to 100% and the others were normalized to this peak. Data acquisition and processing were performed with TOPSPIN software.

**Crystallisation and data collection**

Initial crystallization conditions of BC2L-A were screened using The Classics, Classics II and Classics Lite Suites (Qiagen) and Additive Screen HT (Hampton Research). After condition and concentration refinement, freeze-dried BC2L-A was dissolved in water (7.5 mg/ml) with the presence of 2 mM αMeHep. Single crystals were obtained using the hanging drop method by mixing 1.8 µl of protein solution with 2.2 µl of 0.2 M ammonium sulfate, 30% PEG 8000, 10 mM calcium chloride. Crystals were cryo-cooled after soaking them in 50% PEG 400 mixed with precipitant solution. Diffraction data were collected at beamline ID23-2 (ESRF) showing an orthorhombic $C222_1$ space group with five monomers of lectin per asymmetric unit. The x-ray structure was determined by molecular replacement using Phaser (McCoy *et al.*, 2007) and the BC2L-A monomer as search model (PDB code 2VNV, with removal of ligands and water molecules) (Table 1). After the addition of 10 calcium ions, five αMeHep monomers, 11 sulfate ions and 112 water molecules, the structure was refined using Refmac (Murshudov *et al.*, 1997), alternated to manual rebuilding in Coot (Emsley and Cowtan, 2004) and deposited in the PDB with the accession number 4OAC.

**Titration microcalorimetry**

Freeze-dried BC2L-A was dissolved in 0.1 M Tris/HCl, 500 µM $CaCl_2$, pH 7.5 and equilibrated at room temperature for 1 hour before ITC measurement. All experiments were performed on VP-ITC or ITC200 (GE Healthcare) at 25 °C. Concentration of BC2L-A varied from 0.2 to 0.5 mM, and sugars were used in concentrations 1.5-10 mM according to their binding affinity. Control experiments performed by injections of buffer in the protein solution yielded insignificant heats of dilution. Integrated heat effects were analysed by non-linear regression using a single site-binding model (Microcal Origin 7). Fitted data yielded the association constant ($K_a$) and the enthalpy of binding ($\Delta H$). Other thermodynamic parameters, i.e. changes in free energy, $\Delta G$, and entropy, $\Delta S$, were calculated from equation

$$\Delta G = \Delta H - T\Delta S = -RT\ln K_a$$

where $T$ is the absolute temperature and $R$ = 8.314 $J.mol^{-1}.K^{-1}$. Usually, two to three independent titrations were performed for each ligand tested**.**

## Microscopy

### *BC2L-A labeling*

Freeze-dried lectin BC2L-A was dissolved in 50 mM borate buffer (pH = 8.5) to a final concentration of 2 mg/ml (0.5 mg in 0.25 ml of buffer). FITC (fluorescein 5-isothiocyanate, Sigma-Aldrich) was dissolved in DMF to a concentration of 10 mg/ml and added to the lectin solution in a 20:1 molar ratio ($n_{FITC}$:$n_{lectin}$). The solution was immediately stirred and incubated for 1 hour in the dark at room temperature. Subsequently the excess and hydrolyzed FITC was removed by dialysis against $H_2O$ (at 4 °C with a daily change for three days), volume of the dialysis solution was 4000 times higher than the amount of protein solution (250 µl in 1 l). The lectin-FITC solution was stored at 4 °C in the dark.

### *Cell cultures and staining*

*B. cenocepacia* CCM 4899 (LMG 16656, J. Govan J2315, Czech Collection of Microorganisms, Brno) and *Escherichia coli* BL21(DE3) were cultivated overnight in Luria-Bertani (LB) medium at 37 °C with shaking. 100 µl of overnight culture was centrifuged and cells were washed with buffer (0.1 M Tris/HCl, 500 µM $CaCl_2$, pH 7.5). Cells were incubated with 20 µg/ml BC2L-A-FITC for 30 minutes at 17 °C in dark. Afterwards, cells were thoroughly washed, resuspended in buffer and examined by microscope. For preparation of mixed sample, *B. cenocepacia* and *E. coli* cells were mixed in 1:1 ratio and processed together. For biofilm production, *B. cenocepacia* was cultivated in LB medium at 37 °C with shaking for approximately three days. Biofilm appeared on a glass surface of cultivation flask. Biofilm was scrubbed off and processed as mentioned above. Alternatively, biofilm was grown directly on microscope slides. Slides were submerged to high OD culture of *B. cenocepacia* and cells were cultivated at 37 °C without shaking for two days. Biofilm appeared on a slide as a thin line at the level of LB. Slide was thoroughly washed; biofilm was covered by BC2L-A-FITC and incubated as mentioned previously.

### *Microscope analysis*

5-20 µl of liquid samples or slide with attached biofilm were used for observation. Examination was carried out using motorized inverted fluorescence microscope IX81 (Olympus). Blue light (470-495 nm) was used for FITC excitation and green fluorescence was

observed (575-625 nm). Images were obtained by microscope digital camera DP72 (Olympus).

**Acknowledgements**

A.M., P.K., A.S., A.I. acknowledge the COST action BM1003 "Microbial cell surface determinants of virulence as targets for new therapeutics in Cystic Fibrosis". A.M., A.S. acknowledge PRIN/MIUR 2008/2009 (A.M. and A.S.) and FFC grant 11#2010 with the contribution of Pastificio Giovanni Rana s.p.a (A.M.). P.K. acknowledges funding by Austrian Science Fund (FWF grant P 22909 N-17). A.I. acknowledges the Association Vaincre la Mucoviscidose. .L.M., L.A, M.W acknowledge Czech Science Foundation (303/09/1168) and CEITEC - Central European Institute of Technology with research infrastructure supported by the project CZ.1.05/1.1.00/02.0068 from European Regional Development Fund. Crystal data collection was performed at the European Synchrotron Radiation Facility.

**Abbreviations**

STD: Saturation Transfer Difference; L,D-Hep: L-*glycero*-D-*manno*-heptose; LPS : lipolysaccharide

## References


Agrawal P, Kumar S, Jaiswal YK, Das HR, Das RH. 2011. A Mesorhizobium lipopolysaccharide (LPS) specific lectin (CRL) from the roots of nodulating host plant, *Cicer arietinum*. *Biochimie*. 93:440-449.

Artner D, Stanetty C, Mereiter K, Zamyatina A, Kosma P. 2011. Crystal and molecular structure of methyl L-glycero-alpha-D-manno-heptopyranoside, and synthesis of 1-->7 linked L-glycero-D-manno-heptobiose and its methyl alpha-glycoside. *Carbohydr Res*. 346:1739-1746.

Brimacombe JS, Kabir AKMS. 1986. Convenient syntheses of L-glycero-D-manno-heptose and D-glycero-D-manno-heptose. *Carbohydr Res*. 152:329-334.

Chemani C, Imberty A, de Bentzman S, Pierre P, Wimmerová M, Guery BP, Faure K. 2009. Role of LecA and LecB lectins in *Pseudomonas aeruginosa* induced lung injury and effect of carbohydrates ligands. *Infect Immun*. 77:2065-2075.

Dam TK, Brewer CF. 2002. Thermodynamic studies of lectin-carbohydrate interactions by isothermal titration calorimetry. *Chem Rev*. 102:387-429.

De Castro C, Sturiale L, Parrilli M. 2004. Characterisation of the alpha(1 -> 3) homopolymer of L-glycero-D-manno-heptose units isolated from the O-chain polysaccharide of Agrobacterium radiobacter *Eur J Org Chem*. 2436-2440.

De Soyza A, Silipo A, Lanzetta R, Govan JR, Molinaro A. 2008. Chemical and biological features of *Burkholderia cepacia* complex lipopolysaccharides. *Innate Immun*. 14:127-144.

Emsley P, Cowtan K. 2004. Coot: model-building tools for molecular graphics. *Acta Crystallogr D Biol Crystallogr*. 60:2126-2132.

Gilboa-Garber N. 1982. *Pseudomonas aeruginosa* lectins. *Methods Enzymol*. 83:378-385.

Govan JR, Deretic V. 1996. Microbial pathogenesis in cystic fibrosis: mucoid *Pseudomonas aeruginosa* and *Burkholderia cepacia*. *Microbiol Rev*. 60:539-574.

Holst O. 2007. The structures of core regions from enterobacterial lipopolysaccharides - an update. *FEMS Microbiol Lett*. 271:3-11.

Ierano T, Silipo A, Sturiale L, Garozzo D, Brookes H, Khan CM, Bryant C, Gould FK, Corris PA, Lanzetta R, Parrilli M, De Soyza A, Molinaro A. 2008. The structure and proinflammatory activity of the lipopolysaccharide from *Burkholderia multivorans* and the differences between clonal strains colonizing pre and posttransplanted lungs. *Glycobiology*. 18:871-881.

Imberty A, Varrot A. 2008. Microbial recognition of human cell surface glycoconjugates. *Curr Opin Struct Biol*. 18:567-576.

Imberty A, Wimmerova M, Mitchell EP, Gilboa-Garber N. 2004. Structures of the lectins from *Pseudomonas aeruginosa*: Insights into molecular basis for host glycan recognition. *Microb Infect*. 6:222-229.

Imberty A, Wimmerova M, Sabin C, Mitchell EP. 2006. Structures and roles of *Pseudomonas aeruginosa* lectins. The Royal Society of Chemistry. In Bewley, C (ed), Protein-Carbohydrate Interactions in Infectious Disease. The Royal Society of Chemistry, Cambridge, pp. 30-48.

Jaipuri FA, Collet BY, Pohl NL. 2008. Synthesis and quantitative evaluation of Glycero-D-manno-heptose binding to concanavalin A by fluorous-tag assistance. *Angew Chem Int Ed Engl*. 47:1707-1710.

Jayaraman V, Das HR. 1998. Interaction of peanut root lectin (PRA II) with rhizobial lipopolysaccharides. *Biochim Biophys Acta*. 1381:7-11.

Kawasaki N, Kawasaki T, Yamashina I. 1989. A serum lectin (mannan-binding protein) has complement-dependent bactericidal activity. *J Biochem*. 106:483-489.

Kosma P. 2008. Occurrence, synthesis and biosynthesis of bacterial heptoses. *Curr Org Chem*. 12:1021-1039

Lameignere E, Malinovská L, Sláviková M, Duchaud E, Mitchell EP, Varrot A, Šedo O, Imberty A, Wimmerová M. 2008. Structural basis for mannose recognition by a lectin from opportunistic bacteria *Burkholderia cenocepacia*. *Biochem J*. 411:307-318.

Lameignere E, Shiao TC, Roy R, Wimmerová M, Dubreuil F, Varrot A, Imberty A. 2010. Structural basis of the affinity for oligomannosides and analogs displayed by BC2L-A, a *Burkholderia cenocepacia* soluble lectin. *Glycobiology*. 20:87-98.

Marchessault RH, Pérez S. 1979. Conformations of the hydroxymethyl group in crystalline aldohexopyranoses. *Biopolymers*. 18:2369-2374.

Mayer M, Meyer B. 2001. Group epitope mapping by saturation transfer difference NMR to identify segments of a ligand in direct contact with a protein receptor. *J Am Chem Soc*. 123:6108-6117.

McCoy AJ, Grosse-Kunstleve RW, Adams PD, Winn MD, Storoni LC, Read RJ. 2007. Phaser crystallographic software. *J Appl Crystallogr*. 40:658-674.

Meyer B, Peters T. 2003. NMR spectroscopy techniques for screening and identifying ligand binding to protein receptors. *Angew Chem Int Ed Engl*. 42:864-890.

Mitchell E, Houles C, Sudakevitz D, Wimmerova M, Gautier C, Pérez S, Wu AM, Gilboa-Garber N, Imberty A. 2002. Structural basis for oligosaccharide-mediated adhesion of *Pseudomonas aeruginosa* in the lungs of cystic fibrosis patients. *Nature Struct Biol*. 9:918-921.

Murshudov GN, Vagin AA, Dodson EJ. 1997. Refinement of macromolecular structures by the maximum-likelihood method. *Acta Crystallogr D Biol Crystallogr*. 53:240-255.

Ortega X, Silipo A, Saldias MS, Bates CC, Molinaro A, Valvano MA. 2009. Biosynthesis and structure of the *Burkholderia cenocepacia* K56-2 lipopolysaccharide core oligosaccharide: truncation of the core oligosaccharide leads to increased binding and sensitivity to polymyxin B. *J Biol Chem*. 284:21738-21751.

Paulsen H, Wulff A, Brenken M. 1991. Preparation of synthetic antigens of the inner core region of lipopolysaccharides by copolymerisation with acrylamide. *Liebigs Ann Chem*. 1127-1145.

Pokorná M, Cioci G, Perret S, Rebuffet E, Kostlánová N, Adam J, Gilboa-Garber N, Mitchell EP, Imberty A, Wimmerová M. 2006. Unusual entropy driven affinity of *Chromobacterium violaceum* lectin CV-IIL towards fucose and mannose. *Biochemistry*. 45:7501-7510.

Reiter A, Zamyatina A, Schindl H, Hofinger A, Kosma P. 1999. Synthesis of *Pseudomonas aeruginosa* lipopolysaccharide core antigens containing 7-O-carbamoyl-L-glycero-alpha-D-manno-heptopyranosyl residues. *Carbohydr Res*. 317:39-52.

Silipo A, Molinaro A. 2010. The diversity of the core oligosaccaride in lipopolysaccharides in Endotoxins: structure, function and recognition. *Subcell Biochem*. 53:69-99.

States DJ, Hberkorn RA, Ruben DJ. 1982. A two-dimensional nuclear Overhauser experiment with pure absorption phase in four quadrants. *J Magn Reson*. 48:286-292.

Sudakevitz D, Kostlanova N, Blatman-Jan G, Mitchell EP, Lerrer B, Wimmerova M, Katcof fDJ, Imberty A, Gilboa-Garber N. 2004. A new *Ralstonia solanacearum* high affinity mannose-binding lectin RS-IIL structurally resembling the *Pseudomonas aeruginosa* fucose-specific lectin PA-IIL. *Mol Microbiol*. 52:691-700.

Šulák O, Cioci G, Delia M, Lahmann M, Varrot A, Imberty A, Wimmerová M. 2010. A TNF-like trimeric lectin domain from *Burkholderia cenocepacia* with specificity for fucosylated human histo-blood group antigens. *Structure*. 18:59-72.

Šulák O, Cioci G, Lameignère E, Balloy V, Round A, Gutsche I, Malinovská L, Chignard M, Kosma P, Aubert F, Marolda CL, Valvano MA, Wimmerová M, Imberty A. 2011. *Burkholderia cenocepacia* BC2L-C is a super lectin with dual specificity and proinflammatory activity *PLoS Pathog*. 7:e1002238.

Wang H, Head J, Kosma P, Brade H, Muller-Loennies S, Sheikh S, McDonald B, Smith K, Cafarella T, Seaton B, Crouch E. 2008. Recognition of heptoses and the inner core of bacterial lipopolysaccharides by surfactant protein D. *Biochemistry*. 47:710-720.

**Legends for Figures**

**Scheme 1:** Schematic representation of heptose and derivatives.

**Figure 1:** a) Reference $^{1}$H NMR spectrum and b) STD 1D NMR spectrum of BC2L-A – D-mannose mixture, 1:60; on resonance irradiation frequency at 0.54 ppm, saturation time of 1.5 seconds. c) Epitope mapping of the mannose in the binding site of BC2L-A.

**Figure 2:** a) Reference $^{1}$H NMR spectrum and b) STD 1D NMR spectrum of BC2L-A/αMeHep **2** mixture, 1:60; on resonance irradiation frequency at 0.54 ppm, saturation time of 2.5 seconds. c) Epitope mapping of the αMeHep **2** in the binding site of BC2L-A.

**Figure 3:** a) Reference $^{1}$H NMR and b) STD 1D NMR spectra of BC2L-A/Hepα1-3Hep-O-All **4** disaccharide mixture, 1:60; on resonance irradiation frequency at 7.5 ppm ppm, saturation time of 2 seconds. c) Qualitative epitope mapping of Hepα1-3Hep. The STD intensity increases with the color intensity of the circle.

**Figure 4:** (a) representation of ribbon diagram of BC2L-A dimer complexed with αMeHep (sticks) and calcium (spheres). Sulfate ions are represented by sticks. (b) Electron density (1σ = electron per Å$^{2}$) around the αMeHep with hydrogen bonds to amino acids in binding site represented by dashed lines. (c) Superimposition of the five different binding sites observed in the asymmetric unit.

**Figure 5:** Microcalorimetry data. Upper panels: thermogram of monosaccharides, disaccharides, LPS oligosaccharides and polysaccharides titrating BC2L-A. Lower panel: integration of data with curve fitted for "one binding site" model.

**Figure 6:** (a) cells and (b) biofilm on glass slides of *B. cenocepacia* LMG 16656 (J2315) stained by BC2L-A-FITC. Bright field (left), green fluorescence (middle), superimposition (right). Bar 20 μm.

**Table 1**. Data collection and refinement statistics of BC2L-a structure in complex with αMeHep

| | BC2LA/α-L,D-Methyl-Heptoside |
|---|---|
| ***Data collection statistics*** | |
| Beamline | ID23-2 |
| Unit cell (Å) | *a* = 50.00<br>*b* = 185.14<br>*c* = 186.2100 |
| Spacegroup | $C222_1$ |
| Wavelength (Å) | 0.87260 |
| Resolution limit (Å) | 48.27 – 2.70 (2.85 – 2.70)* |
| Total observations | 116137 |
| Unique reflections | 24265 (3427) |
| Completeness | 99.6 (98.2) |
| Multiplicity | 4.8 (4.6) |
| <I>/<σI> | 10.2 (2.9) |
| $R_{merge\ (\%)}$ [b] | 14.1 (51.9) |
| ***Refinement statistics*** | |
| $R_{cryst}$ | 19.2 % |
| $R_{free}$ | 25.3 % |
| RMSD bonds | 0.011 |
| RMSD angles | 1.569 |
| Ramachandran's outliers | 2 |
| Protein atoms | 4576 |
| Ligand atoms | 85 |
| Water atoms | 112 |
| Other atoms | 55 |

* *Values in parenthesis refer to the highest resolution shell.*

$R_{merge} = \sum|I-\langle I\rangle|/|\sum\langle I\rangle|$, $R_{cryst} = (\sum||F_{obs} - F_{calc}||)/(\sum||F_{obs}||)$

**Table 2**: Microcalorimetry data for the interaction of Bc2lA with monosaccharides and disaccharides

| Ligand | $K_A$ ($10^4$ $M^{-1}$) | $K_D$ (μM) | n | -ΔG (kJ/mol) | −ΔH (kJ/mol) | TΔS (kJ/mol) |
|---|---|---|---|---|---|---|
| D-Man[a] | 19.4 | 5.1 | 0.91 | 30.2 | 27.0 | 3.2 |
| αMeMan[a] | 36.4 | 2.7 | 0.83 | 31.8 | 23.0 | 8.8 |
| L,D-Hep | 0.73 +/-0.3 | 137 | 0.91 +/-0.05 | 22.1 | 10.4 +/- 0.7 | 11.7 |
| LαD-MeHep | 1.86 +/-0.09 | 53.8 | 0.79 +/-0.03 | 24.4 | 9.7 +/- 0.2 | 14.7 |
| LαD- AllylHep | 1.35+/-0.01 | 74.1 | 0.94 +/-0.04 | 23.5 | 12.7+/-1.1 | 10.8 |
| D,D-Hep | No binding | | | | | |
| Hep α1-3Hep-*O*-Allyl | 1.41+/-0.01 | 70.7 | 1.07+/-0.05 | 23.7 | 6.9 +/- 0.3 | 16.8 |
| Hep α1-7Hep | 2.29+/-0.07 | 43.8 | 01.11+/-0.02 | 24.9 | 10.5+/- 0.5 | 14.4 |
| Hep α1-7Hep-*O*-Met[b] | 5.5+/-0.3 | 18.3 | 0.87+/-0.09 | 27.0 | 12.6+/- 0.8 | 14.4 |

[a] From (Lameignere *et al.*, 2008)

[b] Large standard deviations and poor reproducibility due to strong cooperative effect.

**Table 3**: Microcalorimetry data for the interaction of Bc2lA with oligosaccharides and polysaccharides

| Ligand | $K_A$ ($10^4$ $M^{-1}$) | $K_D$ (μM) | n | -ΔG (kJ/mol) | −ΔH (kJ/mol) | TΔS (kJ/mol) |
|---|---|---|---|---|---|---|
| Oligosaccharide 1 *B. cenocepacia* | 0.31+/-0.01 | 325 | 1[a] | 19.9 | 10.2 +/-0.4 | 9.7 |
| Oligosaccharide 2 *B. multivorans* | 0.281[b] | 356 | 1[a] | 19.7 | 11.7 | 8.0 |
| Polysaccharide (L,D Hep1-3)n *A. radiobacter* | 26.6[b] | 3.8 | 0.951 | 30.9 | 24.3 | 6.7 |

[a] Stochiometry fixed during the fitting procedure

[b] only one experimental measure

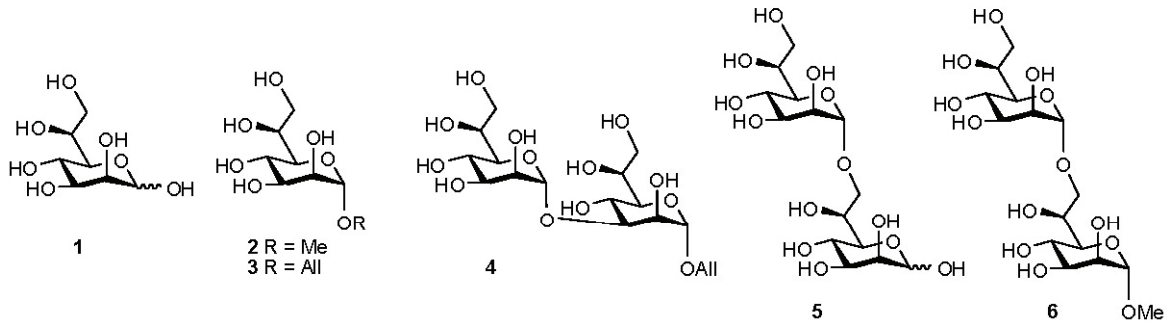


**Oligosaccharide 1** (from *B. cenocepacia* K56-2*Waal* mutant)

L,D-Hep-(1→7)-L,D-Hep-(1→3)-L,D-Hep-(1→5)-D-Kdo
3 4 4
↑ ↑ ↑
1 1 2
L,D-Hep-(1→2)- α-D-Glc β-D-Glc D-Ko-(8←1)Ara4N

**Oligosaccharide 2** (from *Burkholderia multivorans* )

α-L,D-Hep
1
↓
7
β-D-QuiNAc-(1→3)-α-D-Rha-(1→2)-α-L,D-Hep-(1→3)-α-L,D-Hep-(1→5)-α-D-Kdo
3 4 4
↑ ↑ ↑
1 1 2
α-L-Rha β-D-Glc α-D-Ko
3 6
↑ ↑
1 1
β-D-Glc-(1→3)-α-D-GalNAc -(1→3)-β-D-GalNAc α-L,D-Hep

**Polysaccharide** (*Agrobacterium radiobacter*)

$[\alpha\text{-L,D-Hep-}(1\rightarrow3)\text{-}]_n$

**Scheme 1**

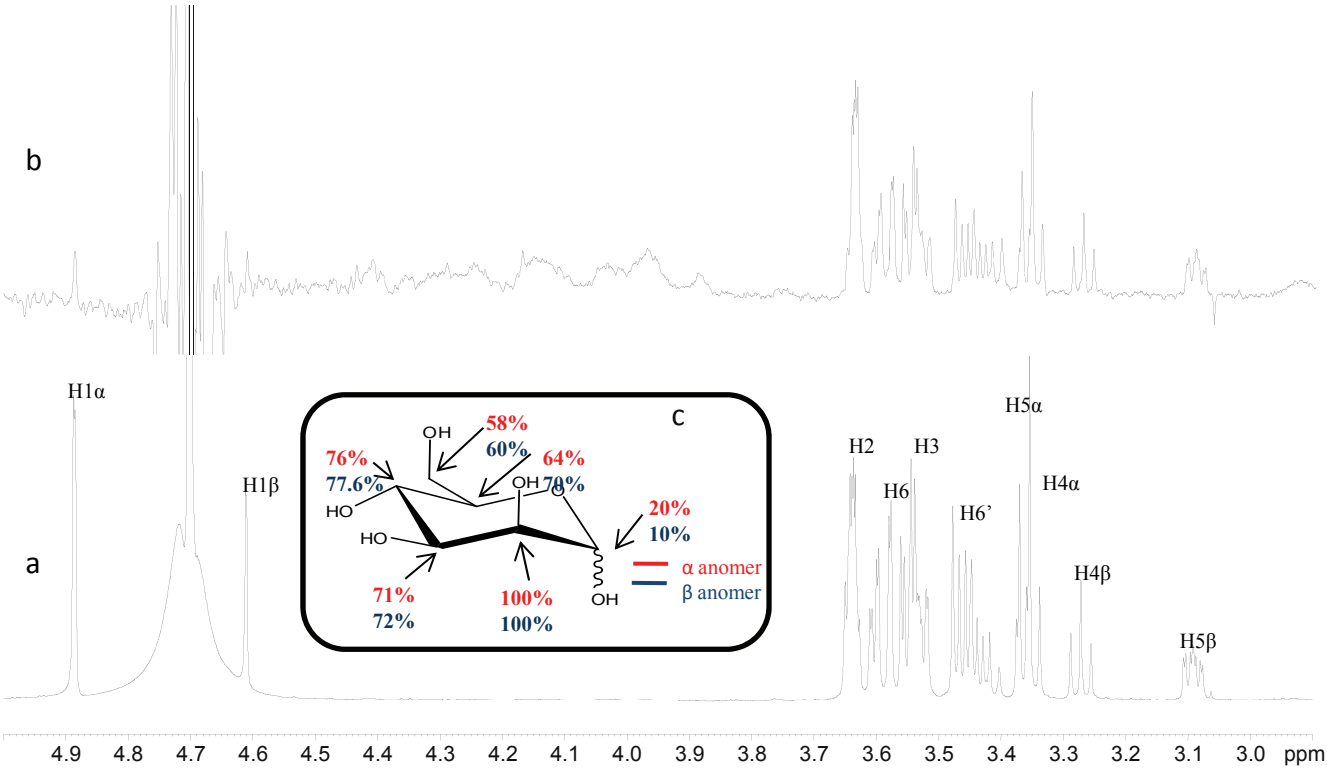
b
a
H1α
H1β
H2
H3
H6
H6'
H5α
H4α
H4β
H5β
c
OH
58%
60%
64%
76%
77.6%
OH
78%
HO
HO
20%
10%
71%
72%
100%
100%
OH
α anomer
β anomer
4.9
4.8
4.7
4.6
4.5
4.4
4.3
4.2
4.1
4.0
3.9
3.8
3.7
3.6
3.5
3.4
3.3
3.2
3.1
3.0
ppm

**Figure 1**

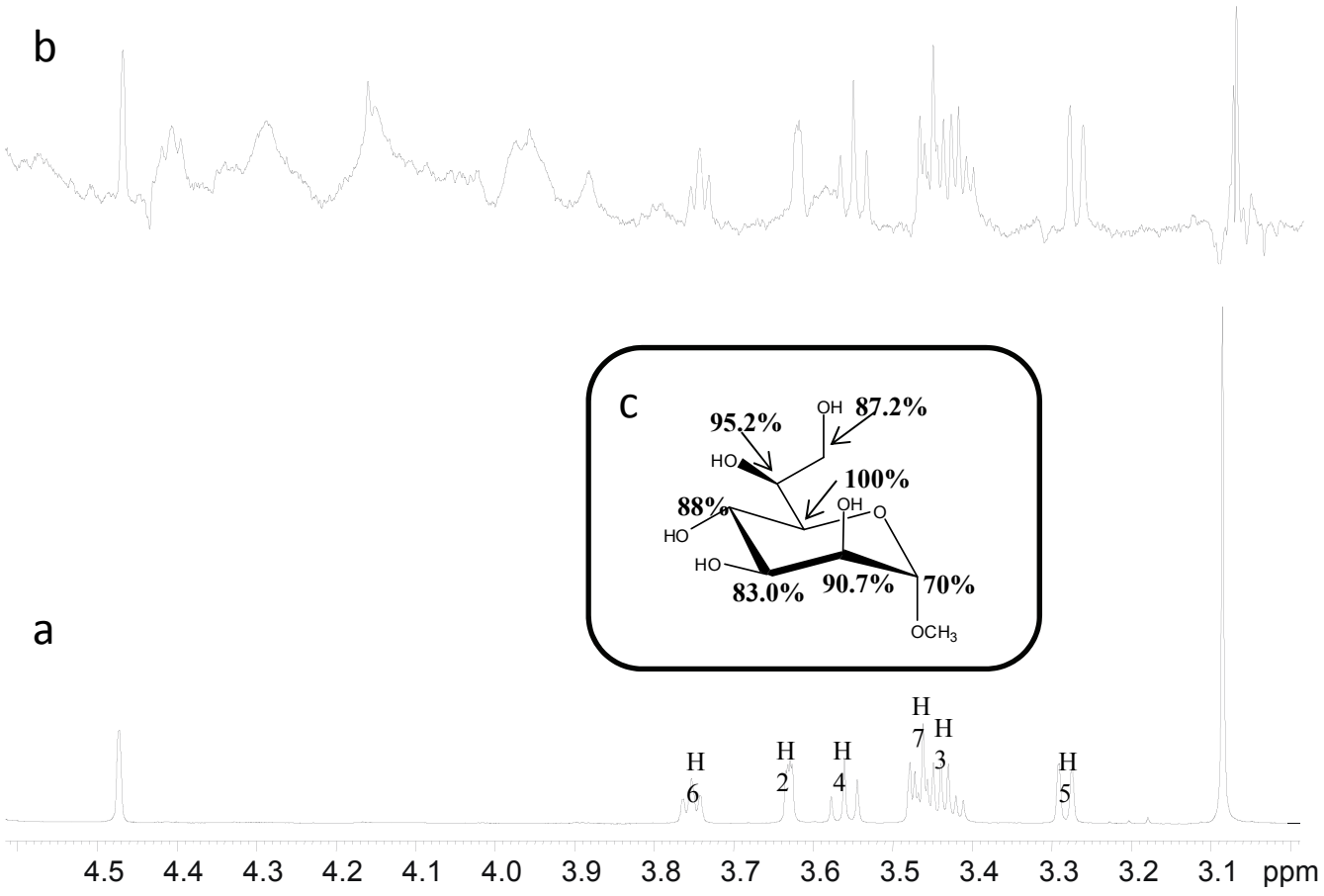
b
a
c
95.2%
OH
87.2%
HO
100%
88%
OH
O
HO
HO
83.0%
90.7%
70%
OCH3
H 6
H 2
H 4
H 7
H 3
H 5
4.5 4.4 4.3 4.2 4.1 4.0 3.9 3.8 3.7 3.6 3.5 3.4 3.3 3.2 3.1 ppm

**Figure 2**

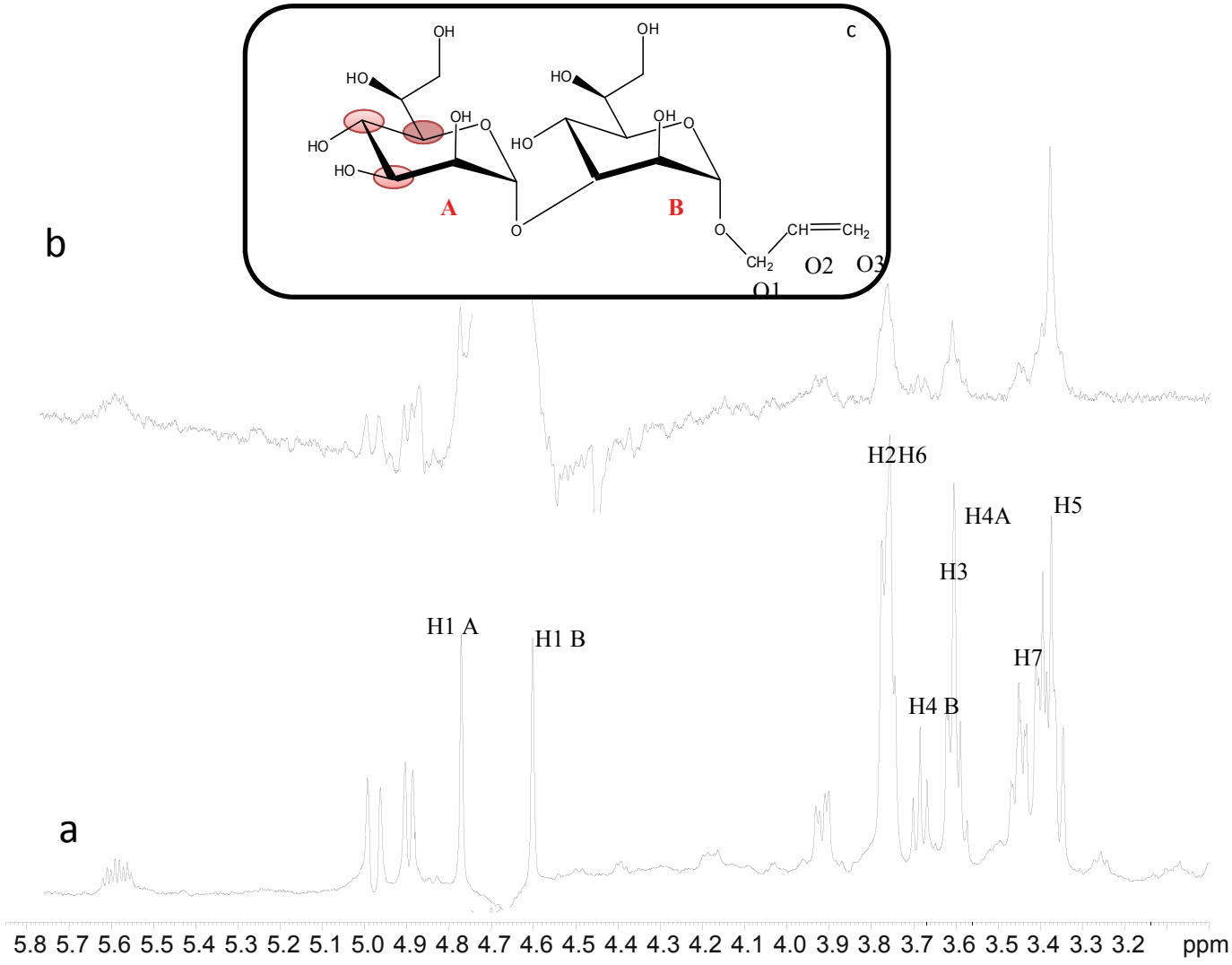
c
OH
HO
OH
O
HO
HO
A
B
O
O
CH
CH2
CH2
O2
O3
O1
b
H2H6
H4A
H5
H3
H1 A
H1 B
H7
H4 B
a
5.8 5.7 5.6 5.5 5.4 5.3 5.2 5.1 5.0 4.9 4.8 4.7 4.6 4.5 4.4 4.3 4.2 4.1 4.0 3.9 3.8 3.7 3.6 3.5 3.4 3.3 3.2
ppm

**Figure 3**

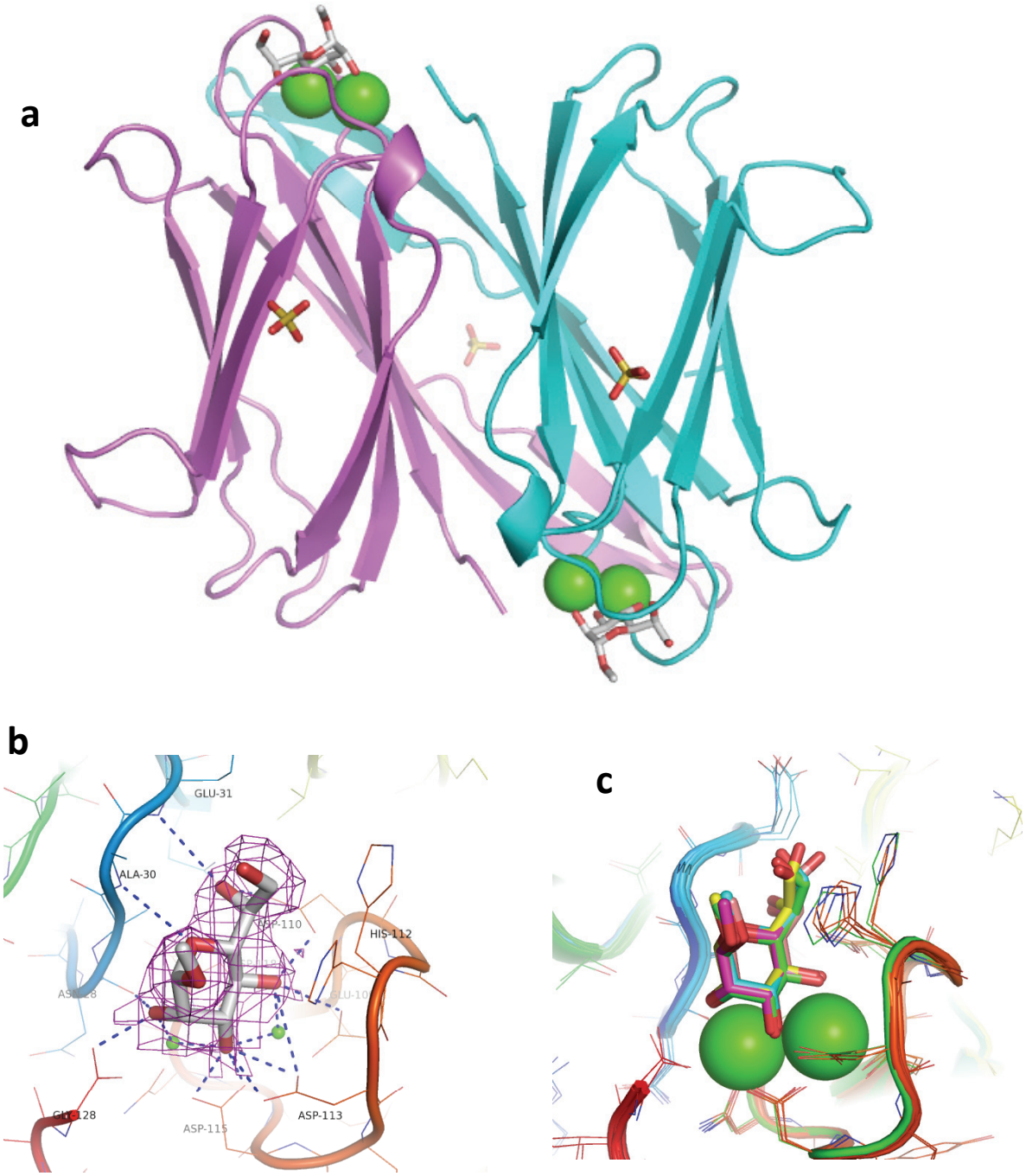


**Figure 4**

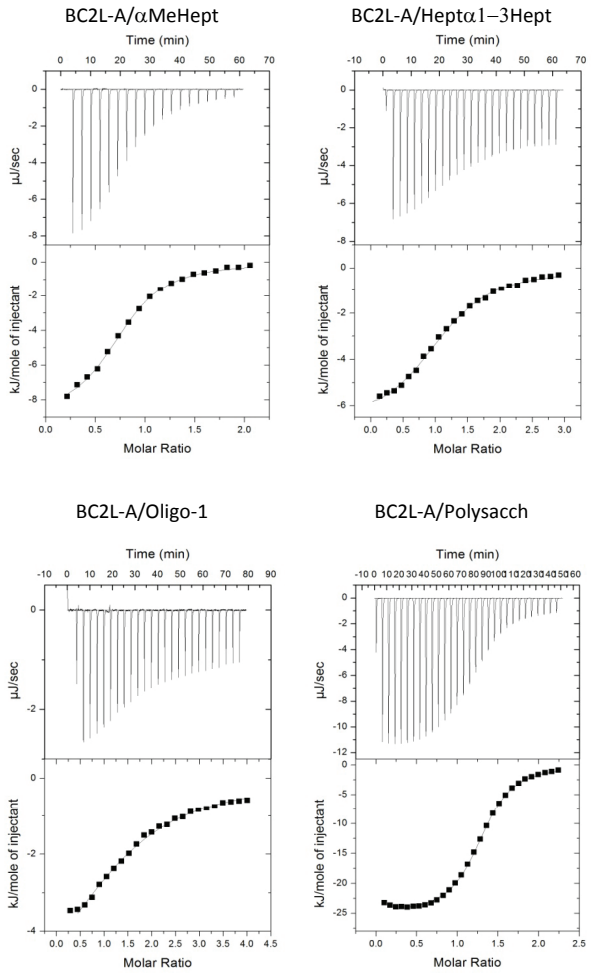
BC2L-A/αMeHept
Time (min)
µJ/sec
kJ/mole of injectant
Molar Ratio
BC2L-A/Heptα1−3Hept
Time (min)
µJ/sec
kJ/mole of injectant
Molar Ratio
BC2L-A/Oligo-1
Time (min)
µJ/sec
kJ/mole of injectant
Molar Ratio
BC2L-A/Polysacch
Time (min)
µJ/sec
kJ/mole of injectant
Molar Ratio

**Figure 5**

a

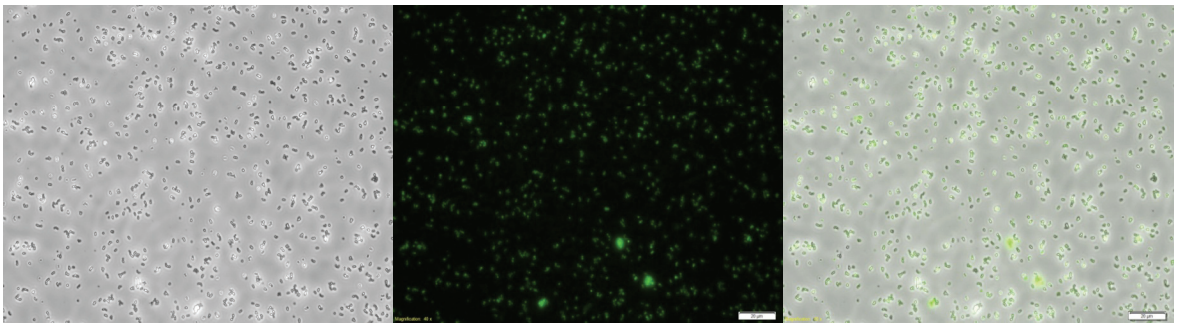

b

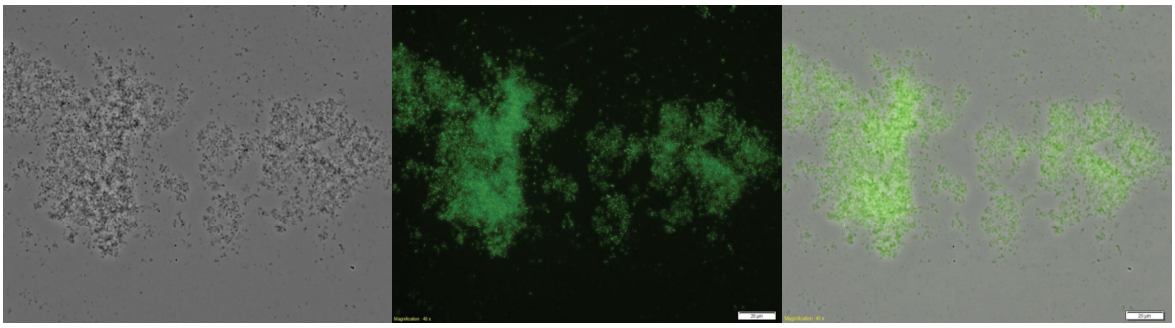

**Figure 6**